

See discussions, stats, and author profiles for this publication at: <https://www.researchgate.net/publication/4351756>

Multiple sliding surface control of idle engine speed and torque reserve with load torque estimation

CONFERENCE PAPER · JULY 2008

DOI: 10.1109/VSS.2008.4570681 · Source: IEEE Xplore

CITATIONS

4

READS

27

4 AUTHORS, INCLUDING:



[Benedikt Alt](#)

Universität der Bundeswehr München

20 PUBLICATIONS 48 CITATIONS

SEE PROFILE



[Ferdinand Svaricek](#)

Universität der Bundeswehr München

75 PUBLICATIONS 160 CITATIONS

SEE PROFILE



[Matthias Schultalbers](#)

56 PUBLICATIONS 133 CITATIONS

SEE PROFILE

Multiple Sliding Surface Control of Idle Engine Speed and Torque Reserve with Load Torque Estimation

Benedikt Alt, Ferdinand Svaricek
University of the German Armed Forces,
Department of Aeronautical Engineering,
Institute of System Dynamics and
Flight Mechanics, 85577 Neubiberg, Germany
benedikt.alt@unibw.de

Jan Peter Blath, Matthias Schultalbers
IAV GmbH, Department of
Powertrain Mechatronics,
Development Gasoline Engines,
38518 Gifhorn, Germany
jan.peter.blath@iav.de

Abstract

A novel controller based on multiple sliding surface control is adopted to automotive engine control at idle condition. The control task is to maintain the engine speed and the torque reserve at their reference values despite parameter uncertainties and variations in the intake-to-torque-production delay. Additionally, a disturbance estimator is applied to reconstruct unknown load torque disturbances based on measurements of the engine speed. A validated nonlinear simulation model is used to evaluate the performance of the closed-loop system and it is shown that the system is robust with respect to the mentioned uncertainties and disturbances.

1. Introduction

The idle speed control (ISC) problem of a spark ignition (SI) engine represents an interesting control design task in the field of automotive engine control. In its simplest form the control target is to hold the engine speed at its desired value despite unknown disturbances. There are two major sources of performance deterioration: On the one hand rapid external load changes result from activating an accessory such as air-conditioning, power steering, battery charging, etc. On the other hand, aging effects due to atmospheric exposure induce long-term variations in the engine parameters and the intake-to-torque-production delay. If the unknown disturbances on the engine speed can be effectively rejected, the driver will have a better impression of the engine quality. Furthermore, the idle speed can be lowered as the load rejection capability is improved. With a lower idle engine speed the fuel consumption can be considerably reduced. Hence, in modern idle speed controls it is a challenging task to find a trade-off between the load rejection capability on the one hand and the fuel consumption on the other hand.

The electronic throttle represents the main input to the idle speed control system. It allows an air stream to enter the engine cylinders. Under the assumption of a fixed stoichiometric air/fuel ratio the engine torque depends on this amount of air in the cylinder. Hence, the electronic throttle is able to set the average engine torque over all cylinders.

Since the air path shows a slow dynamic behaviour, the spark advance is used as second control input. This actuator controls the point of ignition and its setting can be changed on every combustion cycle. At a given operating point the relationship between spark advance and average engine torque reaches a maximum value that is called maximum brake torque T_{max} and the corresponding spark advance setting is called $\alpha_{ign,max}$. The current combustion torque that is also known as indicated torque T_{ind} can be considerably lowered by moving the spark advance away from $\alpha_{ign,max}$. In this case T_{ind} may be increased or even more lowered as seen in Figure 1. Thus, the spark advance set point $\alpha_{ign,SP}$ or as an alternative solution the ignition efficiency

$$\eta_{ign,SP} = \frac{\alpha_{ign,SP}}{\alpha_{ign,max}} \quad (1)$$

allows a fast reaction, however its influence on the torque generation is rather limited compared to the electronic throttle position.

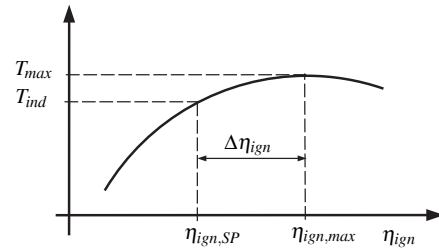


Figure 1. Relationship between engine torque and spark advance at a given operating point

Many current and next generation engine management systems are characterized by a centrally coordinated torque management [1]. This means that all interfaces between the powertrain electronic control units are formulated on a common principle which is based on torques and efficiencies. Hence, this torque structure also has to be considered in the ISC problem. With this the idle speed controller outputs are no longer the physical actuator outputs (throttle position, spark advance). Instead, the two artificial torque demands

T_{air} and T_{ign} of the engine management system represent the new actuator outputs. Furthermore, a second output is introduced besides the engine speed N . This new output is commonly known as torque reserve T_{res} and it describes the offset (in Nm) between the maximum brake torque T_{max} and the indicated torque T_{ind} (see Figure 1). Note that for the ISC problem it is convenient to have a certain torque reserve greater than zero. Otherwise, the spark advance loses its influence on the torque generation of the engine and the system physically depends on the slow dynamics of the electronic throttle. On the other hand a large amount of torque reserve leads to a significant penalty in fuel usage. Hence, it is helpful to design a multiple input multiple output controller with improved disturbance rejection capability that allows holding the engine speed N and the torque reserve T_{res} at their reference values.

Existing production controllers rely on decentralized proportional, integral and differential (PID) controllers with the drawback of time-consuming adjustments to the nonlinear plant. Note that production idle speed controllers are usually characterized by the heuristic settings of the calibration engineer and that there exists no strategy to find an optimum for the trade-off between fuel consumption and load rejection capability. The control parameters for the air path are usually optimized for one specific spark advance setting. If the spark advance is introduced as additional control input a recalibration of the settings for the air path becomes necessary. Hence, the idle speed control problem is still a challenging task in the field of automotive engine control. Unfortunately, many previous control design approaches do not consider the torque structure of modern engine management systems and often it is only shown that the new control design works in a simulation or even on a simplified test rig ([2],[16]), but not within a real series vehicle. Furthermore the throttle position is often the only physical control input and the spark advance is not taken into account.

Nevertheless recent research has applied a wide range of control techniques to the ISC problem. The range goes from linear control techniques valid around an operating point (e.g. modelbased PID-design [3], H_∞ -design [4]) to nonlinear techniques (e.g. feedback linearization [5], neural network based control [8]). Linear control techniques are often combined with gain-scheduling techniques as changes in operating points occur slowly. However heavy loads resulting from an auxiliary accessory can take the engine quickly and significantly away from the nominal operating point. Hence, the nonlinear nature of the plant makes nonlinear synthesis techniques attractive. However the effort for modeling and control design should also be considered. Therefore robust nonlinear control design methods, especially some sliding mode control design techniques become more and more attractive. In the field of sliding mode control (SMC) the method of multiple sliding surface (MSS) control seems very interesting for ISC design since it has been developed for typical applications of automotive engine control ([13, 14, 15]). This method is robust both against matched and unmatched uncertainties and takes care of typical models of automotive systems which contain usu-

ally sparse and experimentally obtained characteristic maps.

The paper consists of three major contributions. First, a mathematical description is developed that takes care of the nonlinear behaviour of the engine at idle, the spark advance as auxiliary input, the centrally coordinated torque management and the torque reserve T_{res} as a new virtual output. Furthermore, this new nonlinear simulation model is validated on a series vehicle. As a second contribution the MSS control design method is adopted to the aforementioned ISC problem. Thus the control design method is applied to a multiple input multiple output problem. A key contribution of this paper is the sliding mode observer based estimation of the unknown load torque T_{load} that results from accessories like the air conditioning, power steering etc. Although the MSS control design is known to be robust against unmatched uncertainties like e.g. the unknown load torque, online estimation of these uncertainties and disturbances could improve the tracking capabilities significantly.

The remainder of this paper is organized as follows. Section 3 gives a brief introduction to the nonlinear simulation model of an SI engine with its engine management system. In section 4 the concept of multiple sliding surface control is adopted to the ISC problem. Section 5 deals with the engine load torque estimation. Nonlinear simulation results are shown in section 6. Finally conclusions are drawn in section 7 and an overview of future work is given.

2. Notation

$\alpha_{ign,SP}$	Spark advance set point [degree]
α_{thr}	Throttle plate position [degree]
$\eta_{ign,SP}$	Ignition efficiency set point [-]
J	Engine moment of inertia [kgm ²]
\dot{m}_{cc}	Mass air flow into the combustion chamber [mg/s]
\dot{m}_{thr}	Mass air flow into the intake manifold [mg/s]
N	Engine speed [1/min]
N_{cc}	Number of cylinders [-]
N_{SP}	Engine speed set point [1/min]
\dot{N}	Rate of change of engine speed [(1/min)/s]
p_{im}	Intake manifold pressure [hPa]
\dot{p}_{im}	Rate of change of intake manifold pressure [hPa/s]
T_{air}	ISC command of the air path [Nm]
T_{drive}	Drive torque at the crankshaft [Nm]
T_{ign}	ISC command of the ignition path [Nm]
T_{ind}	Indicated engine torque [Nm]
T_{load}	Load torque [Nm]
T_{loss}	Friction and pumping losses [Nm]
T_{max}	Maximum brake torque [Nm]
T_{res}	Torque reserve [Nm]
$T_{res,SP}$	Torque reserve set point [Nm]
τ_{thr}	Time constant of the electronic throttle body [s]
τ_d	Intake to torque production delay [s]
θ_{eng}	Temperature of the engine [K]
θ_{im}	Temperature of the air in the intake manifold [K]
V_{im}	Volume of the air in the intake manifold [m ³]
R	Gas constant [287 J/kg/K]

3. Nonlinear engine model

In this section a mathematical model of the engine is introduced. It should serve as a nonlinear simulation model and provides the basis for the control design in section 4. This nonlinear engine model incorporates both the overall system dynamics of the engine and the torque structure of current engine management systems. For the mathematical description of the engine at idle condition it is sufficient to use an approach with a common mean value model ([10, 11]). That means that all processes and effects are spread out over every combustion and differences from cylinder to cylinder are neglected. Furthermore, the engine can be modelled with a time continuous approach. The overall dynamics of the engine are governed by the electronic throttle including its position controller, the intake manifold and the crankshaft with its flywheel inertia. A mathematical description that takes these dynamics into account is given by

$$\dot{\alpha}_{thr} = -\frac{1}{\tau_{thr}}\alpha_{thr} + \frac{1}{\tau_{thr}}\alpha_{thr,u} \quad (2)$$

$$\dot{p}_{im} = \frac{R\theta_{im}}{V_{im}}(\dot{m}_{thr} - \dot{m}_{cc}) \quad (3)$$

$$\dot{N} = \frac{30}{\pi J}(T_{ind} - T_{loss} - T_{load}) \quad (4)$$

where τ_{thr} represents the time constant of the closed loop behaviour of the electronic throttle and $\dot{m}_{thr} = \dot{m}_{thr}(p_{im}, N, T_{air})$ and $\dot{m}_{cc} = \dot{m}_{cc}(p_{im}, N)$ denote the air mass flow rate into the intake manifold and the combustion chamber, respectively. The air mass flow rate into the combustion chamber can also be expressed as flow rate \dot{m}'_{cc} per combustion with

$$\dot{m}'_{cc} = \frac{120}{N_{cc}N}\dot{m}_{cc} \quad (5)$$

The indicated torque $T_{ind} = T_{ind}(\dot{m}'_{cc}(t - \tau_d), T_{ign})$ generated once per combustion is taken as a static function of the air charge \dot{m}'_{cc} into the combustion chamber and of the torque input $T_{ign} = T_{ign}(t - \tau_d)$ of the ignition path where τ_d represents the intake-to-torque-production delay. The indicated torque T_{ind} results from calculations of the engine management system as torque measurements are too expensive for series vehicles. Furthermore, current engine management systems are also able to estimate the friction and pumping losses $T_{loss} = T_{loss}(p_{im}, N)$ of the engine. Nevertheless, there exist some unknown load torque disturbances T_{load} acting directly on the crankshaft dynamics of the engine (e.g. accessories like air conditioning, power steering, etc.). Since the torque structure includes several subordinated feedforward and feedback control loops, these should also be considered in the nonlinear simulation model. Among these control loops the charge controller calculating the setpoint for the throttle position

$$\alpha_{thr,u} = f_1(T_{air}, \dot{m}_{cc,SP}, \dot{m}_{cc}) \quad (6)$$

plays a significant role where

$$\dot{m}_{cc,SP} = f_2(T_{air}, T_{loss}, \eta_{ign,max}, N) \quad (7)$$

denotes the set point of the air mass flow into the combustion chamber. Hence, the physical actuator inputs (throttle position α_{thr} and ignition efficiency set point $\eta_{ign,SP}$) are transformed both into torque demands T_{air} and T_{ign} on the air path and on the ignition path, respectively. With this the torque demand T_{ign} is the only control input acting directly on the indicated torque T_{ind} and hence on the engine speed N at idle. The remaining control input T_{air} on the air path influences the maximum brake torque T_{max} and with

$$T_{res} = T_{max} - T_{ind} \quad (8)$$

it is also able to adjust the torque reserve T_{res} . Hence, there exists a dynamical actuator constraint for T_{ign} and an unidirectional coupling between the two torque demands T_{air} and T_{ign} . Next, the following nonlinear state space representation can be derived from equations (2), (3), (4), (6), (7) and (8):

$$\begin{bmatrix} \dot{\alpha}_{thr} \\ \dot{p}_{im} \\ \dot{N} \end{bmatrix} = \begin{bmatrix} g_1(\alpha_{thr}, p_{im}, N, T_{air}) \\ g_2(\alpha_{thr}, p_{im}, N, T_{air}) \\ g_3(\alpha_{thr}, p_{im}, N, T_{ign}) \end{bmatrix} \quad (9)$$

$$\begin{bmatrix} N \\ T_{res} \end{bmatrix} = \begin{bmatrix} x_3 \\ h_2(\alpha_{thr}, p_{im}, N, T_{air}, T_{ign}) \end{bmatrix} \quad (10)$$

where $\mathbf{x} = [\alpha_{thr} \ p_{im} \ N]^T$, $\mathbf{u} = [T_{air} \ T_{ign}]^T$ and $\mathbf{y} = [N \ T_{res}]^T$.

Hence, the nonlinear model from equations (9) and (10) represents the base for the application of modelbased control theory.

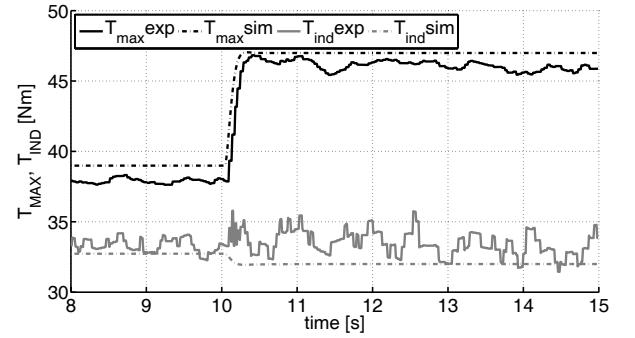


Figure 2. Maximum brake torque and indicated torque: Comparison of the experimental data with the simulation after a step in the torque demand on the air path

In the following the nonlinear mathematical description of the engine has to be validated on the real plant. For this purpose a representative validation procedure has been carried out on a series vehicle with a 2.0l spark ignition engine using a common rapid control prototyping system. Figure 2 shows as an example an acceptable matching between the simulation model and the real plant after a step in the torque demand T_{air} on the air path.

4. Multiple sliding surface control

In this section a procedure similar to integrator backstepping ([17]) is adopted to the aforementioned idle speed control problem. This method is called Multiple Sliding Surface (MSS) control and it has been developed to simplify controller design of systems where model differentiation is difficult and where the matching condition is not fulfilled ([13, 14, 15]). This section adopts this method to the problem of holding the engine speed N and the torque reserve T_{res} at their reference values. For general information about MSS control design the reader is referred to [15]. For the aforementioned idle speed control problem a modular structure with three layers as illustrated in Figure 3 is introduced, including the control of the throttle position α_{thr} , the combined control of the drive torque T_{drive} and the torque reserve T_{res} and finally the control of the idle engine speed N .

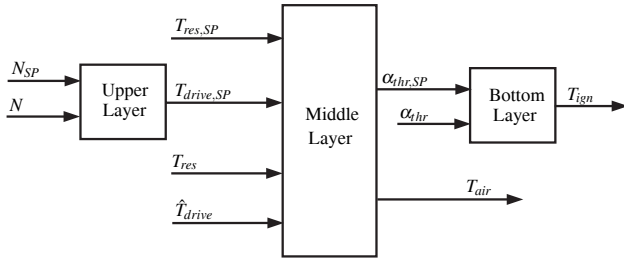


Figure 3. Block diagram of the controller

4.1. Control of throttle position

In the first step the bottom layer of the controller is developed. The task is to generate a torque demand T_{air} on the air path such that the actual throttle position $\alpha_{thr,SP}$ corresponds to its desired value. Hence the sliding surface σ_1 is defined as

$$\sigma_1 = \alpha_{thr} - z = 0 \quad (11)$$

where z is the output of an additional first order lag that provides a continuously differentiable signal of $\alpha_{thr,SP}$:

$$\dot{z} = -\frac{1}{\tau_z}z + \frac{1}{\tau_z}\alpha_{thr,SP} \quad (12)$$

In the following steps the task is to deduce a control law for the controller output T_{air} . For this purpose the time derivative of equation (11)

$$\dot{\sigma}_1 = \alpha_{thr}' - \dot{z} \quad (13)$$

has to be calculated. To make the sliding surface σ_1 attractive its time derivative should satisfy

$$\dot{\sigma}_1 = -K_{d1}\text{sat}(\sigma_1) \quad (14)$$

Hence, the right hand sides of equations (13) and (14) can be equated. Under the assumption that the static function

of $\alpha_{thr,u}$ in equation (6) depends primarily on the torque demand T_{air} this relationship can be inverted and the following assumption is justified:

$$T_{air} \approx f_1^{*(-1)}(\alpha_{thr,u}) \quad (15)$$

Together with equations (2) and (15) the controller output T_{air} can be derived and it is given by

$$T_{air} = f_1^{*(-1)}\left(\tau_{thr}\left(\frac{1}{\tau_{thr}}\alpha_{thr} + \frac{1}{\tau_z}\alpha_{thr,SP} - \frac{1}{\tau_z}z - K_{d1}\text{sat}(\sigma_1)\right)\right)$$

To prove the stability of the resulting closed loop system, the η -reachability condition

$$\sigma_1 \dot{\sigma}_1 \leq -\eta |\sigma_1| \quad (16)$$

has to be satisfied where $\eta > 0$ is an arbitrary constant. To satisfy equation (16) system uncertainties have to be incorporated as far as possible. One of these bounded uncertainties is the closed loop time constant τ_{thr} of the electronic throttle with its position controller

$$\frac{1}{F_{thr}} \leq \frac{\tau_{thr}}{\hat{\tau}_{thr}} \leq F_{thr} \quad (17)$$

where F_{thr} represents the aforementioned uncertainty bound. Furthermore, the assumption of equation (15) leads to the second source for the bounded uncertainties:

$$\frac{1}{F_1} \leq \frac{f_1}{\hat{f}_1} \leq F_1 \quad (18)$$

Under consideration of the bounds of the system uncertainties the switching gain K_{d1} can be calculated as

$$K_{d1} \geq F_1 \tau_{thr} \eta + (F_1 \tau_{thr} - 1) \frac{1}{\tau_z} (\alpha_{thr,SP} - z) \quad (19)$$

and thus the time taken to reach the sliding surface $\sigma_1 = 0$ is given by

$$t_{sm} \leq \frac{|\sigma_1(0)|}{\eta} \quad (20)$$

Hence, the asymptotic stability can be guaranteed if condition (19) is satisfied.

4.2. Control of drive torque and torque reserve

In the next step the middle layer of the controller is developed. For this purpose the relevant nonlinear state space representation can be deduced from equations (9) and (10) and it is given by

$$\begin{bmatrix} \dot{p}_{im} \\ \dot{N} \end{bmatrix} = \begin{bmatrix} g_{21}(p_{im}, N) + g_{22}(T_{air}) \\ g_{31}(p_{im}, N) + g_{32}(T_{ign}) \end{bmatrix} \quad (21)$$

$$\begin{bmatrix} T_{drive} \\ T_{res} \end{bmatrix} = \begin{bmatrix} h_1(\alpha_{thr}, p_{im}, N, T_{air}, T_{ign}) \\ h_2(\alpha_{thr}, p_{im}, N, T_{air}, T_{ign}) \end{bmatrix} \quad (22)$$

The task is to generate both torque demands T_{air} and T_{ign} on the air path and on the ignition path in a way that the

drive torque $T_{drive,SP}$ and the torque reserve $T_{res,SP}$ correspond to their desired values. The design of the middle layer of the controller is split into two separate tasks. In the first step a control law is developed that generates the torque demand T_{ign} . In the second step a control law is developed which generates the desired value of the throttle position $\alpha_{thr,SP}$ which serves as reference value for the bottom layer of the controller.

For the first design step two sliding surfaces σ_{21} and σ_{22} have to be defined:

$$\begin{aligned}\sigma_{21} &= T_{drive} - T_{drive,SP} = 0 \\ \text{and } \sigma_{22} &= T_{res} - T_{res,SP} = 0.\end{aligned}\quad (23)$$

The controller output T_{ign} is calculated by means of the time derivatives of the sliding surfaces σ_{21} and σ_{22} :

$$\begin{aligned}\dot{\sigma}_{21} &= \dot{T}_{drive} - \dot{T}_{drive,SP} \\ \text{and } \dot{\sigma}_{22} &= \dot{T}_{res} - \dot{T}_{res,SP}\end{aligned}\quad (24)$$

where \dot{T}_{drive} and \dot{T}_{res} have to be calculated by means of the total derivatives of T_{drive} and T_{res} :

$$\begin{aligned}\dot{T}_{drive} &= \frac{\partial h_1}{\partial p_{im}} \dot{p}_{im} + \frac{\partial h_1}{\partial N} \dot{N} + \frac{\partial h_1}{\partial T_{air}} \dot{T}_{air} + \frac{\partial h_1}{\partial T_{ign}} \dot{T}_{ign} \\ \dot{T}_{res} &= \frac{\partial h_2}{\partial p_{im}} \dot{p}_{im} + \frac{\partial h_2}{\partial N} \dot{N} + \frac{\partial h_2}{\partial T_{air}} \dot{T}_{air} + \frac{\partial h_2}{\partial T_{ign}} \dot{T}_{ign}.\end{aligned}$$

From simulation studies it is known that $\frac{\partial h_i}{\partial N} \ll \frac{\partial h_i}{\partial p_{im}}$ and $\frac{\partial h_i}{\partial T_{air}} \ll \frac{\partial h_i}{\partial T_{ign}}$ for $i = 1, 2$. Hence the corresponding partial derivatives in equation (24) can be neglected. Since both sliding surfaces σ_{21} and σ_{22} have to be driven simultaneously to zero their time derivatives have to be incorporated both into the calculation of the control law for T_{ign} . Hence $\dot{\sigma}_{21}$ and $\dot{\sigma}_{22}$ have to be added to a combined time derivative:

$$\begin{aligned}\dot{\sigma}_{21} + \dot{\sigma}_{22} &= \left(\frac{\partial h_1}{\partial p_{im}} + \frac{\partial h_2}{\partial p_{im}} \right) \dot{p}_{im} \\ &\quad + \left(\frac{\partial h_1}{\partial T_{ign}} + \frac{\partial h_2}{\partial T_{ign}} \right) \dot{T}_{ign} - \dot{T}_{drive} - \dot{T}_{res}\end{aligned}$$

To make both sliding surfaces attractive their time derivatives should satisfy

$$\dot{\sigma}_{21} = \sum_{i=1}^2 \dot{\sigma}_{21i} \text{ and } \dot{\sigma}_{22} = \sum_{i=1}^2 \dot{\sigma}_{22i} \quad (25)$$

where

$$\sum_{i=1}^2 \dot{\sigma}_{21i} = -K_{d21} \text{sat}(\sigma_{21}) - K_{l21} \sigma_{21} \quad (26)$$

and

$$\sum_{i=1}^2 \dot{\sigma}_{22i} = -K_{d22} \text{sat}(\sigma_{22}) - K_{l22} \sigma_{22}. \quad (27)$$

Hence the right hand sides of equations (25), (26) and (27) can be equated. Consequently the torque input T_{ign} on the ignition path can be deduced and it is given by

$$\begin{aligned}T_{ign} &= T_{ign}(0) + \int \left(\frac{\partial h_1}{\partial T_{ign}} + \frac{\partial h_2}{\partial T_{ign}} \right)^{-1} \left(- \left(\frac{\partial h_1}{\partial p_{im}} + \frac{\partial h_2}{\partial p_{im}} \right) \dot{p}_{im} \right. \\ &\quad \left. + \sum_{i=1}^2 \dot{\sigma}_{21i} + \sum_{i=1}^2 \dot{\sigma}_{22i} + \dot{T}_{drive,SP} + \dot{T}_{res,SP} \right) dt.\end{aligned}$$

The stability proof is not printed due to space constraints but it is similar to section 4.1. In the following the second design step of the middle layer of the controller is explained. The task is to develop a control law that generates the desired value of the throttle position $\alpha_{thr,SP}$ and to take the control law for the torque demand T_{ign} on the ignition path into consideration, too. In particular, the fast dynamics of the torque demand T_{ign} should be taken into account and this should be the essential controller output for transient reactions. Hence, a new sliding surface

$$\sigma_{31} = T_{ign} - T_{ign,SP} = 0 \quad (28)$$

can be defined and it should be quickly driven to zero. Furthermore, two more sliding surfaces

$$\begin{aligned}\sigma_{32} &= T_{drive} - T_{drive,SP} = 0 \\ \text{and } \sigma_{33} &= T_{res} - T_{res,SP} = 0\end{aligned}\quad (29)$$

have to be defined in order that the desired values of the drive torque $T_{drive,SP}$ and the torque reserve T_{res} correspond to their desired values. Since $\sigma_{32} = \sigma_{21}$ and $\sigma_{33} = \sigma_{22}$ the calculation of the corresponding time derivatives

$$\begin{aligned}\dot{\sigma}_{31} &= \dot{T}_{ign} - \dot{T}_{ign,SP}, \\ \dot{\sigma}_{32} &= \dot{T}_{drive} - \dot{T}_{drive,SP} \text{ and} \\ \dot{\sigma}_{33} &= \dot{T}_{res} - \dot{T}_{res,SP}\end{aligned}\quad (30)$$

is similar to equation (24). Thus, a new combined time derivative

$$\begin{aligned}\dot{\sigma}_{31} + \dot{\sigma}_{32} + \dot{\sigma}_{33} &= \dot{T}_{ign} - \dot{T}_{ign,SP} + \left(\frac{\partial h_1}{\partial p_{im}} + \frac{\partial h_2}{\partial p_{im}} \right) \dot{p}_{im} \\ &\quad + \left(\frac{\partial h_1}{\partial T_{ign}} + \frac{\partial h_2}{\partial T_{ign}} \right) \dot{T}_{ign} - \dot{T}_{drive} - \dot{T}_{res}\end{aligned}$$

can be calculated. To make all three sliding surfaces attractive their time derivatives should satisfy

$$\dot{\sigma}_{31} = 0, \dot{\sigma}_{32} = \sum_{i=1}^2 \dot{\sigma}_{32i} \text{ and } \dot{\sigma}_{33} = \sum_{i=1}^3 \dot{\sigma}_{33i} \quad (31)$$

where

$$\dot{T}_{ign} = \dot{T}_{ign,SP} = 0, \quad (32)$$

$$\sum_{i=1}^2 \dot{\sigma}_{32i} = -K_{d32} \text{sat}(\sigma_{32}) - K_{l32} \sigma_{32}^3 \quad (33)$$

and

$$\sum_{i=1}^3 \dot{\sigma}_{33i} = -K_{d33} \text{sat}(\sigma_{33}) - K_{l33} \sigma_{33} - K_{i33} \int \sigma_{33} d\tau. \quad (34)$$

Hence, the right hand sides of equations (30), (31), (33) and (34) can be equated. Consequently, the desired value $\alpha_{thr,SP}$ for the bottom layer of the controller can be deduced and it is given by

$$\alpha_{thr,SP} = f_1^{*(-1)} \left(g_{22}^{*(-1)} \left(-g_{21}^* + \left(\frac{\partial h_1}{\partial p_{im}} + \frac{\partial h_2}{\partial p_{im}} \right)^{-1} (\dot{T}_{drive,SP} + \dot{T}_{res,SP} + \left(\frac{\partial h_1}{\partial T_{ign}} + \frac{\partial h_2}{\partial T_{ign}} \right) \dot{T}_{ign} + \sum_{i=1}^2 \dot{\sigma}_{32i} + \sum_{i=1}^3 \dot{\sigma}_{33i}) \right) \right) .$$

As mentioned before the stability proof for the middle layer of the controller runs similarly to section 4.1. and it is also not printed due to space constraints.

4.3. Control of idle engine speed

The following section deals with the upper layer of the controller. The control task is to develop a control law that generates a desired value of the drive torque $T_{drive,SP}$ that serves as reference value for the middle layer of the controller. As the idle engine speed N should correspond to a predefined reference value N_{SP} a new sliding surface

$$\sigma_4 = N - N_{SP} = 0 \quad (35)$$

can be defined. The reference value for the middle layer of the controller $T_{drive,SP}$ is calculated by means of the time derivative of equation (35):

$$\dot{\sigma}_4 = \dot{N} - \dot{N}_{SP} . \quad (36)$$

To make the sliding surface σ_4 attractive its time derivative should satisfy

$$\dot{\sigma}_4 = \sum_{i=1}^3 \dot{\sigma}_{4i} \quad (37)$$

where

$$\sum_{i=1}^3 \dot{\sigma}_{4i} = -K_{d4} \text{sat}(\sigma_4) - K_{l4} \sigma_4 . \quad (38)$$

Together with equation (4) the desired value for the drive torque $T_{drive,SP}$ can be deduced and it is given by

$$T_{drive,SP} = \frac{\pi J}{30} \left(\dot{N}_{SP} + \sum_{i=1}^3 \dot{\sigma}_{4i} \right) . \quad (39)$$

The stability proof for the upper layer of the controller runs similarly to section 4.1. and it is also not printed due to space constraints.

5. Load torque estimation

The last control design step deals with the estimation of the unknown load torque disturbances T_{load} that result from an accessory like air conditioning, power steering, etc. Due to the fact that the load torque acts like an unmatched disturbance on the engine it should be estimated on-line from measurements of the idle engine speed N . With the estimation of the unknown load torque T_{load} the load rejection and tracking capabilities of the idle speed controller can be considerably improved ([18]). From [19] various techniques for

on-line input estimation are known. Thus, the load torque T_{load} can be estimated with a Luenberger observer, a dirty differentiator, a high gain observer or even with a sliding mode observer. Due to robustness issues the two latter solutions seem to be adequate for the incorporation into the idle speed controller of an SI engine. In this work the unknown load torque T_{load} is estimated using a sliding mode observer. From equation (4) the relationship

$$\dot{\xi} = T_{ind} - T_{loss} - T_{load} \quad (40)$$

can be deduced where $\xi = \frac{J\pi}{30}N$. Now the task is to estimate T_{load} from the measurements of ξ , T_{ind} and T_{loss} . For this purpose a further sliding surface $\sigma_5 = 0$ is introduced where $\sigma_5 = \xi - \hat{\xi}$ and $\hat{\xi}$ represents the estimate of the variable ξ . Furthermore, the following variable structure filter

$$\dot{\hat{\xi}} = T_{ind} - T_{loss} - \gamma \text{sat}(\sigma_5) \quad (41)$$

is introduced with $\gamma > 0$. The unknown load torque T_{load} is calculated by means of the time derivative of the sliding surface

$$\dot{\sigma}_5 = \dot{\xi} - \dot{\hat{\xi}} . \quad (42)$$

Together with equations (40) and (41) the time derivative of the sliding surface σ_5 can be deduced and is given by

$$\dot{\sigma}_5 = -T_{load} + \gamma \text{sat}(\sigma_5) . \quad (43)$$

As the aim of this load torque estimation is to drive the error between the variable ξ and its estimate $\hat{\xi}$ to zero as quick as possible the time derivative of the sliding surface σ_5 should satisfy $\dot{\sigma}_5 = 0$. Hence, the unknown load torque T_{load} can be estimated with

$$\hat{T}_{load} = -\gamma \text{sat}(\sigma_5) . \quad (44)$$

To remove the high frequency oscillations from the estimated load torque \hat{T}_{load} a first order lag is introduced with

$$\dot{\hat{T}}_{load,f} = \gamma (-\hat{T}_{load} + \gamma \text{sat}(\sigma_5)) . \quad (45)$$

Finally, the asymptotic stability of the sliding mode observer is considered. From [19] it is known that for any $t \geq t_{sm}$ with $t_{sm} = \frac{2}{\gamma} |\sigma_5(0)|$ the system is said to be in sliding mode on the sliding surface $\sigma_5 = 0$ if the parameter γ satisfies the condition $\gamma > b + \frac{\gamma}{2}$ whereas $\sup |T_{ind} - T_{loss}| \leq b$ represents the upper bound of the difference between the indicated torque T_{ind} and the torque losses T_{loss} . Note that T_{ind} and T_{loss} are calculated values of the engine management system. Furthermore, it is known from [19] that the estimation error between ξ and $\hat{\xi}$ is upper bounded and is

$$|\sigma_5(t)| \leq \sqrt{\sigma_5(0)^2 e^{-\gamma t} + \frac{b^2}{\gamma^2}} . \quad (46)$$

6. Nonlinear simulation results

This section illustrates the efficiency and the robustness properties of the proposed control framework. The following simulations are carried out with the validated nonlinear simulation model of section 2 with a sample time of

$t_s = 10$ ms. Firstly, the disturbance rejection capabilities are demonstrated. For this purpose an additional load torque of $T_{load} = 10$ Nm is applied to the engine at $t_1 = 15$ s and removed at $t_2 = 25$ s.

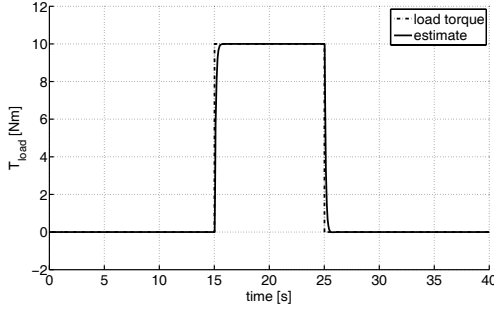


Figure 4. Estimation of the unknown load torque

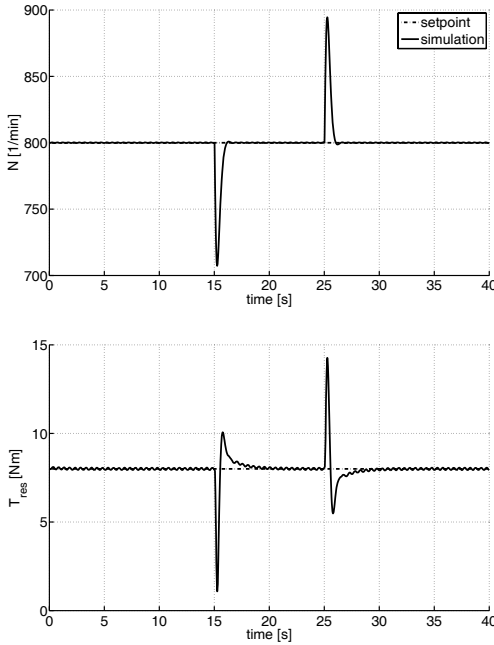


Figure 5. Engine speed and torque reserve: Disturbance rejection capabilities with unknown load torque

In Figure 4 it can be seen that the sliding mode observer presented in section 5 is able to calculate an accurate estimate \hat{T}_{load} of the applied load torque using measurements of the engine speed N and estimates of the indicated torque T_{ind} and the torque losses T_{loss} . Furthermore, it is shown in Figure 5 that the proposed MSS controller of section 4 is able to hold the engine speed N and the torque reserve T_{res} at their reference values while the unknown load torque T_{load} is applied to the engine. In Figure 6 a change in the reference value of the engine speed N_{SP} is introduced. It can be reasoned that the settling times are reasonable small and the

overshoot is negligible.

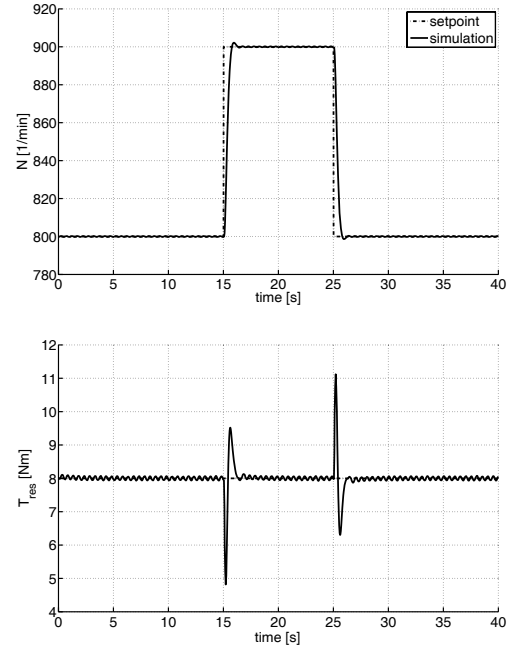


Figure 6. Engine speed and torque reserve: Changing reference value of the idle engine speed

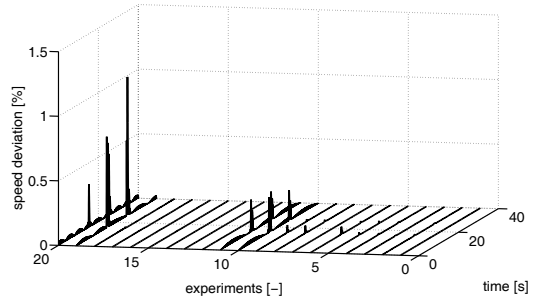


Figure 7. Relative engine speed error: Robustness analysis with uncertainties in the system parameters and in the intake-to-torque-production delay

Finally, selected results of a robustness analysis are given in Figure 7. In this analysis up to 19 different model parameters and characteristic maps of the nonlinear simulation model are varied by $\pm 10\%$ around its nominal value. Furthermore, the intake to torque production delay has been increased by 400 %. For all these variations the engine speed N and the torque reserve T_{res} are considered both together with the aforementioned disturbance rejection scenario and also with the change in the reference value of the engine speed N_{SP} . The deviation to the corresponding nominal engine speed and torque reserve shown in Figures 5 and 6 is normalized around the operating point

($N_{SP0} = 800$ 1/min, $T_{res,SP0} = 8$ Nm). The resulting relative engine speed error is shown for 20 variations with strongest impact on the system. It can be reasoned that the relative engine speed error is bounded with about 1 % in the transient phase of the disturbance rejection scenario.

7. Conclusion and future work

This paper deals with the problem of holding the idle engine speed and the torque reserve at their reference values despite unknown load torque disturbances and system uncertainties. In the first step a nonlinear plant description is introduced that contains the underlying physical relationships of an SI engine. Furthermore, the torque structure of current engine management systems is considered and the nonlinear si-mulation model is validated on a series vehicle. For holding the engine speed and the torque reserve at their reference values a multiple sliding surface design controller is introduced. This control framework consists of three layers and two control laws that generate the torque demands on the air path and the ignition path. Furthermore, the influence of load torque disturbances that act as unmatched disturbances on the system is minimized using a sliding mode observer for load torque estimation. The resulting control framework is able to handle the whole operating range at idle with unchanged control gains. Hence, it is simple to calibrate and can be easily adopted if changes in the plant occur. The efficiency and the robustness against system uncertainties and variations in the intake-to-torque-production delay is shown by nonlinear simulation results.

The ongoing and future work consists in the implementation of the proposed control framework on a series vehicle. In particular, robustness has to be analyzed on the real plant and the new control framework has to be compared with the production controller regarding design and calibration effort, control performance and robustness properties. Additionally, the authors research interest tends to methods for adaptive calibration for the control gains in order to further reduce design and calibration effort.

8. References

- [1] Gerhardt, J., N. Benninger and W. Hess, "Torque based system structure of an electronic engine management system (ME7) as a new base for drivetrain systems", *Proceedings of the FISITA Congress*, Paris, France, 1998, Paper F98T624.
- [2] Bhatti, A.I., S.K. Spurgeon, R. Doorey and C. Edwards, "Sliding mode configurations for automotive engine control", *Int. J. Adapt. Control Signal Process.*, vol. 13, 1999, pp 49-69.
- [3] Böhme, T. and O. Kurdi, "Tuning of an PID based idle speed controller for heavy load rejection using a model-based optimization methodology", *Proceedings of the 2006 IEEE Conference on Computer Aided Control Systems Design*, Munich, Germany, 2006.
- [4] Bohn, C., T. Böhme, A. Staate and P. Mannemann, "A nonlinear model for design and simulation of automotive idle speed control strategies", *Proceedings of the 25th American Control Conference*, Minneapolis, USA, 2006.
- [5] Pfiffner, R. and L. Guzzella, "Feedback linearization of a multi-input SI-engine system for idle speed control", *Proceedings of the 5th IEEE Mediterranean Conference on Control and Systems (MED)*, Paphos, Cyprus, 1997, Paper MP4-2.
- [6] Alt B., Blath J.P., Otto K.-D., Svaricek F. and M. Schultalbers, "Observer-based output tracking of engine speed and torque reserve at idle with sliding mode control", *Proceedings of the European Control Conference*, Kos, Greece, 2007.
- [7] Butts, K.R., N. Sivashankar and J. Sun, "Application of l_1 optimal control to the engine idle speed control problem", *IEEE Transactions on Control Systems Technology*, vol. 7(2), 1999, pp 258-269.
- [8] Li, X. and N. S. Yurkovich, "Neural network based, discrete adaptive sliding mode control for idle speed regulation in IC engines", *Journal of Dynamic Systems, Measurement and Control*, vol. 122, 2000, pp 269-275.
- [9] Ford, R. and K. Glover, "Spark ignition engine idle speed control using a novel framework and enabling control of the tradeoff between fuel consumption and load rejection capability", *Vehicle System Dynamics*, vol. 36(2-3), 2001, pp 225-251.
- [10] Hrovat, D. and J. Sun, "Models and control methodologies for IC engine idle speed control design", *Control Engineering Practice*, vol. 5, 1997, pp 1093-1100.
- [11] Guzzella, L. and C.H. Onder, *Introduction to Modelling and Control of Internal Combustion Engine Systems*, Springer-Verlag, Heidelberg, Germany, 2004.
- [12] Utkin, V.I., "Variable structure systems with sliding modes", *IEEE Transactions on Automatic Control* Vol. 22, 212-222, 1977.
- [13] Green, J. and J.K. Hedrick, "Nonlinear speed control for automotive engines", *Proceedings of the American Control Conference*, San Diego, CA, Vol. 3, pp. 2891-2898.
- [14] Won, M. and J.K. Hedrick, "Multiple-surface sliding control of a class of uncertain nonlinear systems", *International Journal of Control*, Vol. 64, pp. 693-706, 1996.
- [15] Hedrick J.K. and P.P. Yip, "Multiple sliding surface control: theory and application", *Transactions of the ASME*, Vol. 122, pp 568-593, 2000.
- [16] Edwards, C. and S.K. Spurgeon, *Sliding Mode Control, Theory and Applications*, Taylor and Francis LTD, London, 1998.
- [17] Krstic, M., Kanellakapoulous, I. and P. Kokotovic, *Nonlinear and adaptive control design*, Wiley Interscience, New York, 1995.
- [18] Stotsky, A., Eghardt, B. and S. Eriksson, "Variable structure control of engine idle speed with estimation of unmeasurable disturbances", *Journal of dynamic Systems, Measurement and Control*, Vol. 122, pp. 599-603, 2000.
- [19] Stotsky, A. and I. Kolmanovsky, "Simple unknown input estimation techniques for automotive applications", *Proceedings of the American Control Conference*, Arlington, VA, pp. 3312-3317.